RELATIVE PERMEABILITY IN TIGHT GAS SANDSTONE RESERVOIRS - THE "PERMEABILITY JAIL" MODEL

Robert M. Cluff, The Discovery Group Inc., 1560 Broadway Ste 1470, Denver, Colorado, USA
Alan P. Byrnes, Kansas Geological Survey at the University of Kansas, now with Chesapeake Energy Corporation, 6100 N. Western Avenue, Oklahoma City, Oklahoma, 73118 USA

Copyright 2010, held jointly by the Society of Petrophysicists and Well Log Analysts (SPWLA) and the submitting authors.

This paper was prepared for presentation at the SPWLA 51st Annual Logging Symposium held Perth, Australia, June 19-23, 2010.

ABSTRACT

Permeability Jail is a useful concept for explaining typical two-phase (gas-water) relative permeability behavior in tight gas sandstone reservoirs. Although the basic behavior is typical of any two-phase flow system, where one fluid phase interferes with the ability of the other phase to flow freely, the combination of small pore throats in tight gas reservoirs with a reactive, polar, liquid phase (water) leads to some surprises.

The concept of Permeability Jail was first developed in 1992 during an unpublished multi-client study of Mesaverde tight gas sandstones in the eastern Green River Basin of the U.S. Although used informally for over a decade, the idea was not published until 2004 as part of a larger conceptual study of low-permeability reservoir systems. The basic notion is that in tight rocks there exists a saturation region in which the relative permeabilities to both gas and water are so low that neither phase has any effective flow capacity. Because each phase blocks the other from moving, it appears the formation is completely locked up and the fluids are in Jail. We have only observed this phenomena in very low permeability formations, typically with absolute gas permeabilities less than 50 micro-Darcies (<0.05 mD), and we define Jail as the region with <2% Krg and <2% Krw. Therefore the effective permeabilities to both phases are below 1 micro-Darcy. The Jail region varies by rock type and specifics of the pore geometry, but roughly occurs in the 55%-80% Sw range. Tighter rocks tend to have broader Sw range in Jail. Jail does not exist in more permeable rocks because the cross-over point between the gas and water relative permeability curves is at a higher Kr, often 5% or higher, such that one or the other or both phases can establish continuous tendrils through the rock and flow at measureable rates over the entire saturation range. Jail occurs because water is tightly held by capillary forces in the small pore throats of a tight gas sandstone, blocking the flow of gas through those throats, while at the same time the amount of free water connected through those same throats is extremely low and discontinuous over more than a few pore lengths. It is the absence of larger pore throats that are not completely blocked by pendular water that prevents the flow of gas through a rock in Jail.

INTRODUCTION

Industry assessment of the regional low-permeability gas resource, projection of future gas supply, and exploration programs require an understanding of reservoir properties and accurate tools for formation evaluation. As the permeability of the reservoir decreases, the need for progressively more advanced and expensive stimulation technology (e.g., massive hydraulic fractures, multistage fractured horizontal wells) increases and the requirement for accurate estimation of reservoir properties increases. For low-permeability sandstones (and carbonates, though not discussed in this paper) effective gas permeability is strongly influenced by confining stress, saturation, and saturation history and data presented here indicate that the influence of these variables increases with decreasing permeability.

The concept of Permeability Jail was first developed in 1992 during an unpublished multi-client study of Mesaverde low-permeability (tight) gas sandstones in the eastern Green River Basin of the U.S. Although used informally for over a decade, the idea was not published until 2004 as part of a larger conceptual study of low-permeability reservoir systems. The basic notion is that in tight rocks there exists a saturation region in which the relative permeabilities to both gas and water are so low that neither phase has any effective flow capacity with respect to flow rates measured in commercial or laboratory time frames. Because each phase blocks the other from moving, it appears the formation is completely locked up and the fluids are in "Jail." We have only observed this phenomena in very low permeability formations,

typically with absolute gas permeabilities less than 50 micro-Darcies (<0.05 mD), and we define Jail as the region with <2% Krg and <2% Krw. Therefore the effective permeabilities to both phases are below 1 micro-Darcy. The Jail region varies by rock type and specifics of the pore geometry, but generally occurs in the 55%-80% Sw range. Data, presented here, support the interpretation that rocks can be put into Jail as the result of drainage relative permeability conditions, imbibition trapping, or drainage-imbibition hysteresis. Examination of a typical evolution of tight sandstone during burial and diagenesis predicts conditions that would lead to Jail for portions of the gas column and are consistent with the observed long transition zone for tight gas sandstones.

This paper will review studies and data that support a model of low-permeability sandstone permeability and relative permeability that predicts the presence of a gas-water saturation region where the effective permeability to both phases is very low (relative permeability < 2%) and that the range of saturations over which this region exists expands as the permeability decreases. The paper will review key concepts and finding concerning low-permeability rock stress dependence and drainage- and imbibition- relative permeability that lead to the condition of low effective permeability to both phases that is informally refered to as "Permeability Jail."

Though portions of many low-permeability reservoir systems are in Permeability Jail, it is important to note that what might be informally interpreted as "Jail" in one economic setting may be relative freedom in a different setting. These differences are explored.

TIGHT SANDSTONE PERMEABILITY STRESS DEPENDENCE AND PORE ARCHITECTURE

To understand tight gas sandstone properties it is necessary to understand their pore geometry (architecture).

In most low-permeability sandstones and siltstones, routine air permeability values range from 10 to 100 times greater than *in situ* gas and liquid permeability values (Fig. 1). Previous studies of low-permeability sandstones and siltstones have shown that the difference between permeabilities measured at routine conditions and those measured at confining stress increases progressively with decreasing permeability and increasing confining pressure (Vairogs et al, 1971; Thomas and Ward, 1972; Byrnes et al, 1979; Jones and Owens, 1980; Ostensen, 1983; Walls et al, 1982; Sampath and Keighin, 1981; Wei et al, 1986; Luffel et al, 1991; Byrnes, 1997; Castle and Byrnes, 1998; Byrnes and Castle, 2000; Byrnes, 2003; Byrnes, 2005).

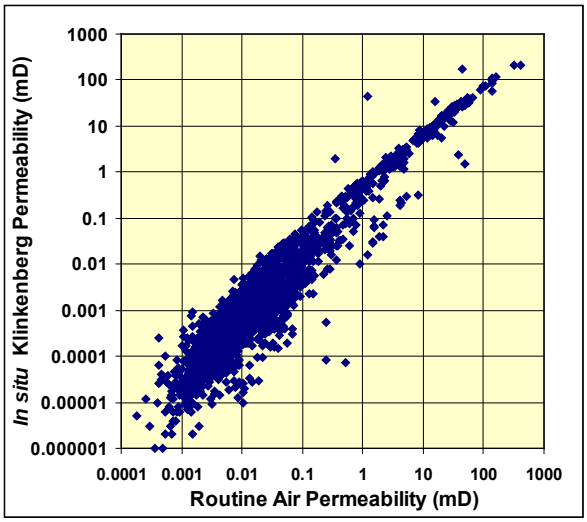

Fig. 1. *In situ Klinkenberg permeability (as measured at 4,000 psi net effective stress) versus routine air permeability (as measured at 100 psi mean pore pressure and 800 psi net effective stress) for Mesaverde Fm sandstones of Western US. (After Byrnes et al, 2009)*

In a key study, Jones and Owens (1980) quantified these effects and concluded that the presence of a thin, sheet-like, tabular pore structure could explain the response to confining stress. This result was consistent with the modeling work of Cheng and Toksoz (1979). Ostensen (1983) provided a comprehensive theoretical analysis of the relationship between crack or thin sheet-like pore permeability and the response of rock properties to confining stress.

The thin-tabular pores measured by capillary pressure methods represent the pore throats in tight gas sandstones and generally exhibit threshold entry equivalent radii of 0.1-1 microns (μm). Assuming an approximate range in pore throat sizes over the entire saturation range of the rock to "irreducible saturation of 10X, the pore throat sizes range from 0.01 μm to 1 μm. The principal pore volume in these rocks is represented by interparticle pores and, commonly, large secondary pores developed in dissolved feldspar and lithic grains. This pore architecture can be broadly characterized as large (10-100 μm) interparticle and intraparticle pore bodies separated by thin tabular (0.01-1 μm) pore throats. This architecture plays an important part in both the drainage and imbibition relative permeability curves.

DRAINAGE GAS RELATIVE PERMEABILITY

We can characterize the gas flow aspect of Permeability Jail by examining the properties of gas relative permeability curves for low-permeability rocks. Relative gas permeability (k_{rg}) data for low-permeability sandstones have been reported in numerous studies (Thomas and Ward, 1972; Byrnes et al., 1979; Jones and Owens, 1980; Sampath and Keighin, 1981; Walls, 1981; Walls et al., 1982; Randolph, 1983; Ward and Morrow, 1987; Chowdiah, 1987; Kamath and Boyer, 1995; Byrnes, 1997; Castle and Byrnes, 1998, 2005; Byrnes and Castle, 2000; Byrnes, 2003, 2005; Shanley et al., 2004; Byrnes 2008, Byrnes et al, 2009). Some k_{rg} measurements have been performed at water saturations (S_w) less than the saturation at which water may be "immobile" under a pressure gradient, and by definition, water relative permeability is zero. In the laboratory these sub-S_{wc} saturations were usually achieved by evaporation. Such saturations may or may not also exist in nature where Pressure-Volume-Temperature-Composition-time (PVTXt) changes to the fluids and rock can potentially reduce water saturations below S_{wc}.

Byrnes et al. (1979) utilized a modified-Corey (1954) equation to predict gas relative permeability in low-permeability sandstones:

$$k_{rg}=(1-(S_w-S_{wc})/(1-S_{gc}-S_{wc}))^p(1-((S_w-S_{wc})/(1-S_{wc}))^q) \quad [1]$$

where S_w is water saturation, S_{cg} is the critical gas saturation, S_{wc} is the critical water saturation, and p and q are exponents, which Corey assigned to have a value of 2. Assigning p = 2 and q = 2 to generally model theoretical and observed data, Corey noted that p and q can change with pore structure. Brooks and Corey (1966) more thoroughly investigated the nature of pore-size distribution influence on relative permeability. They also noted that the Corey- or Brooks-Corey type equations are not defined at water saturations greater than S_{gc} and less than S_{wc} even though "minor" flow may exist in these saturation regions. Issues related to operational, experimental and theoretical definitions of critical saturations underlie many debates about these properties.

The k_{rg} data in the $S_w < S_{wc}$ region exhibit continuity with data in the $S_w \geq S_{wc}$ region. To model these data in Corey-type equations, and avoid the apparent contradiction of water saturations below the saturation at which water is immobile, a term $S_{wc,g}$ can be used that defines water saturations specific for gas only. Alternately, the Corey equation S_{wc} value and p exponent can be changed or Boolean expressions could be used to model these conditions. It is important to note that the critical saturations in the Corey equation mathematically define a saturation at which no flow occurs but this is an operational definition that even Corey commented upon in his original paper. The critical saturation is defined as the saturation at which no "significant" flow occurs. The operational definition of significant is tied to the time frame in which flow is measured. Insignificant flow within a laboratory time frame may represent significant flow over geologic time.

Byrnes et al. (1979) modeled k_{rg} data of Mesaverde cores using Equation 1 with S_{gc} = 0.2-0.3, S_{wc} = 0, p = 1.1-1.3, and q = 2. For Mesaverde cores studied by Sampath and Keighin (1981) and Ward and Morrow (1987), reformatted to Equation 1, their equations utilized S_{gc} = 0.3, $S_{wc,g}$ = 0, p = 1.5, and q = 2.

Relative gas permeability data, representing k_{rg} values obtained at a single S_w and k_{rg} values obtained for a single sample at several saturations, were compiled from published studies (Thomas and Ward, 1972; Byrnes et al, 1979; Jones and Owens, 1980; Sampath and Keighin, 1981; Walls, 1981; Ward and Morrow, 1987; Byrnes, 1997; Castle and Byrnes, 1998; Byrnes and Castle, 2000) and from unpublished data (Fig. 2).

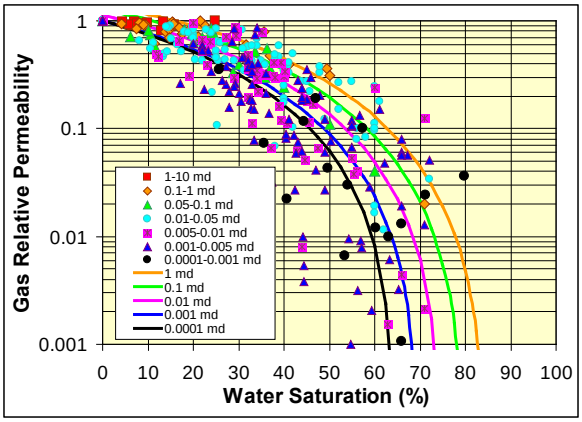

Fig. 2. *Gas relative permeabilities measured at single Sw parametrically with sample k_{ik}. Curves show Corey predicted $k_{rg,Sw}$ values for samples with k_{ik}=0.0001 mD to k_{ik}=1 mD using equations in text.*

Figure 3 illustrates gas relative permeability curves measured on 43 core plug samples at several saturations from seven of the studies cited. In both figures the data have been classified by the absolute permeability of the rock. For most of the studies, water saturations were achieved by both drainage (gas displacement of water) and by evaporation. The curves for all samples tie back to Sw = 0% for the dry samples. The dry gas permeabilities represent the gas or Klinkenberg gas permeability at the confining stress state similar to the confining stress of the $k_{eg,Sw}$ measurements. Thomas

and Ward (1972) reported that confining stress has little effect on k_{rg} but Ward and Morrow (1987) data can be interpreted to indicate that k_{rg} may decrease up to ~10% between low and high confining stress.

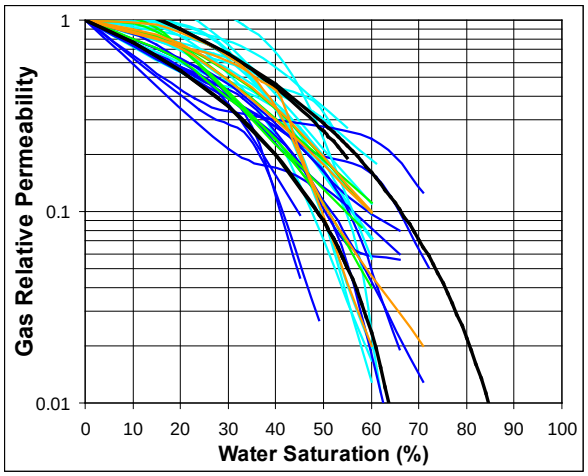

Fig. 3. *Relative gas permeability curves for 43 samples shown parametrically with permeability compiled from seven studies. Curves are separated into k_{ik} < 0.01 mD (dark blue), 0.01< k_{ik} < 0.03 mD (blue), 0.03< k_{ik} < 0.1 mD (green), 0.1< k_{ik} mD (orange). Bounding heavy black curves are derived from the Corey equation model using parameters discussed in the text for k_{ik} = 0.001 mD (lower curve) and k_{ik} = 1 mD (upper curve).*

Figures 2 and 3 can be interpreted to show that at any given S_w, $k_{rg,Sw}$ tends to be lower with decreasing absolute permeability. The data exhibit significant scatter but it is interpreted that a significant influence on the variance is lithologic variability not expressed in the absolute permeability value and that for a single lithology the trends shown would be clearer. The single point data represent over 350 individual sandstone samples exhibiting a very wide range of lithologic (e.g., siltstone to lithic arkose to quartzose sandstone) and bedding (massive to cross-bedded to flaser bedded) properties. The complete k_{rg} curves were measured on a similarly wide range of lithologically diverse sandstones.

The gas relative permeability curves shown in both figures are bounded above and below by Corey-type Eq. 1 with the following parameters:

$S_{wc} = 0.16 + 0.053*\log_{10}k_{ik}$ (where<0 then 0) [2]
$S_{gc} = 0.15 - 0.05*\log_{10}k_{ik}$ [3]
p = 1.7 (to 2.3 depending on lithology and S_{gc}) [4]
q = 2 [5]

where S_{wc} and S_{cg} are expressed in fractions and k_{ik} is expressed in mD. It is important to note that Eqs. 1-5 provide a gas relative permeability that is referenced to the absolute or single phase permeability, such as the *in situ* Klinkenberg gas permeability at S_w = 0.

Assuming the Corey equations presented here are approximately correct, the shift in the position of the k_{rg} curves in Figure 2 can be interpreted to indicate that either S_{gc} increases with decreasing absolute permeability or the Corey exponent increases with decreasing absolute permeability. At high S_w, few data are published but the data and projection of k_{rg} (relative permeability to gas) curves support two Corey-type models: 1) constant k_{rg} exponents (p = 1.7, q = 2) with variable critical gas saturation, and 2) near constant low critical gas saturation with a varied k_{rg} p exponent. Byrnes (2008) reported threshold mercury injection capillary pressure measurements, coupled with electrical resistance measurements on Mesaverde Formation sandstones to measure critical non-wetting (e.g., gas) saturation. He interpreted that the data can be evaluated using four pore network architecture models: 1) percolation (N_p), 2) parallel (N_{II}), 3) series (N_{s1}), and 4) discontinuous series (N_{s2}). Data and analysis suggest that critical gas saturation (S_{gc}) is scale and bedding architecture dependent in cores and in the field. S_{gc} decreases with increasing lattice dimension. S_{gc} is likely to be very low (S_{gc}< 3%) in thinly laminated sandstones where properties vary among beds, low (S_{gc} < 10%) in relatively homogeneous sandstones of any permeability, and may be low to high (10% < S_{gc} < 50%) in heterogeneous lithologies. Results indicate that in heterogeneous lithologies the [p=C; $S_{gc}(k)$] equations, where S_{gc} increases with decreasing k as in Eq. 3, may be more appropriate while in homogeneous lithologies a [$p(k)$; S_{gc}≈C] model may apply, where S_{gc} is constant and low (e.g., S_{gc} < 10%) and the Corey exponent p increases with decreasing k (e.g., 2.5 > p > 1.7 for 0.0001 < k_{ik} < 10). Both approaches can provide identical k_{rg} curves but invoke different mechanisms for why the curve shapes and positions exist. Whichever model is used the shift in the k_{rg} curve to lower S_w with decreasing permeability results in progressively lower effective gas permeabilities with decreasing absolute permeability.

At the S_{wc} end of the relative permeability curve, the data also show that k_{rg} at any given S_w increases with increasing absolute permeability. Higher permeability samples can exhibit k_{rg} at low-moderate S_w (~0-0.2) that are equal to the dry gas permeability at S_w=0. This can result from water occupying pore space that is inconsequential to flow. There is a tendency to assign S_{wc} = 0, as done in the studies cited, because the k_{rg} curve is connected from some low-moderate S_w to the dry k_{rg} value of one. The high k_{rg} values for several

higher permeability samples in this shown here would indicate S_{wc} can be greater than zero.

Eq. 2 predicts $S_{wc} > 0.20$ for higher permeability rocks ($k_{ik} > 10$ mD) and approaches zero with decreasing k_{ik} down to 0.001 mD and below. Eq, 3 predicts $S_{gc} < 0.1$ for higher permeability rocks and approaches $S_{gc} = 0.30$ by $k_{ik} = 0.001$ mD. Taken together these trends imply that as absolute permeability decreases any water in the pore space interferes with gas flow and that greater gas saturation is needed to establish a connective path. These two conditions are consistent. Perhaps most important is that values for S_w at S_{gc} in very low-permeability rocks begin to approach saturations present in the reservoir. This would indicate that these low-permeability rocks have gas saturation but that it is essentially immobile or nearly immobile.

DRAINAGE WATER RELATIVE PERMEABILITY

Having defined the gas relative permeability conditions that can lead to a Jail sentence for gas, we can characterize the water flow aspect of Permeability Jail by examining the properties of water relative permeability curves for low-permeability rocks.

Jones and Owens (1980) reported that water permeability is progressively less than Klinkenberg gas permeability with decreasing permeability for $k_{ik} < 1$ mD following the general equation:

$$k_w = k_{ik}^{1.32} \quad [6]$$

where k_{ik} and k_w are in mD. This trend may be due to the polar nature of water and hydrogen bonding or due to bound water restriction of free-flowing pore cross-sectional area. Given the thin, sheet-like tabular nature of the pore throats in low-permeability sandstones, the influence of even minor water on the width of the tabular pore can be significant. The observed decrease in water permeability is not believed to be due to inert pore-size fluid-flow effects because oil permeabilities are similar to k_{ik} permeabilities (Jones and Owens, 1980). Ward and Morrow (1987) proposed the use of the Corey wetting-phase equation to calculate water relative permeability with values presented relative to k_{ik} by using the ratio of the k_w/k_{ik}:

$$k_{rw} = ((S_w-S_{wc})/(1-S_{wc}))^r \, (k_w/k_{ik}) \quad [7]$$

where r = 4. Implications of Equations 6 and 7 for k_{rw} are significant even with minor variations in S_{wc} and the exponent.

Few data exist in the literature for critical water saturation of low-permeability sandstones. To measure S_{wc} values for Mesaverde sandstones, 1-inch diameter core samples were placed in a Hassler-type cell and subjected to a confining pressure equal to 4,000 psi. Water-saturated air was flowed through the core at an upstream pressure of approximately 1,200 psi with atmospheric downstream pressure. Gas was allowed to flow until effluent water flow was observed to nearly stop. Subsequent to this, effluent water was measured by weight until effluent water flow was less than 0.0001 times gas flow rate at mean pore pressure in the core. This measurement records the critical water saturation as defined by Qg/Qw > 99.99 (where Qg = gas flow and Qw = water flow). This does not measure the saturation at which water flow is zero but is consistent with immobile water for "commercial" flow rates. It is recognized that capillary end effect on the cores results in elevated water saturations at the down-stream end of the core, but the purpose of this test was not to measure the gas permeability but to displace water to S_{wc}.

Low-permeability gas sandstones are typically characterized by high capillary pressure and high S_{wi}. Correlations of S_{wi} with porosity and permeability provide a useful model for approximate S_{wi} prediction or alternately capillary pressure properties can be modeled (Byrnes, 1997; Byrnes and Castle, 2000). For the Medina Formation quartzose and arkosic sandstones and the Mesaverde-Frontier Formation (Mesa-Frnt) lithic sandstones S_{wi} exhibits good correlation with porosity:

$$\log_{10}S_{wi} = -0.97 \log_{10}\phi_i + 2.06 \quad \text{Medina} \quad [8]$$
$$\log_{10}S_{wi} = -0.80 \log_{10}\phi_i + 2.23 \quad \text{Mesa-Frnt} \quad [9]$$

where S_{wi} and ϕ_i are in percent. For both the Medina and the Mesaverde-Frontier sandstones, S_{wi} increases sharply with decreasing porosity below 6-8%. S_{wi} exhibits markedly lower values for ϕ_i greater than 8% in the Medina and for ϕ_i greater than 10% in the Mesaverde-Frontier. Reduced major axis analysis of the relationship between S_{wi} and k_i for Medina and Mesaverde-Frontier sandstones yields the relationship:

$$\log_{10}S_{wi} = -0.187 \log_{10}k_{ik} + 1.18 \quad [10]$$

where S_{wi} is in percent and k_{ik} is in mD. Taking the capillary measured "irreducible" water saturation and the gas displacement critical water saturation, S_{wc} decreases with increasing permeability, and is always greater than water saturation obtained at air-brine capillary pressure equal to 300 psi (Fig. 4). Correlation between S_{wc} and "S_{wi}" exhibits a linear trend that can be characterized by the equation:

$S_{wc} = 0.68\ S_{wi} + 38$ [11]

where S_{wc} and S_{wi} are in percent. The difference between S_{wc} and S_{wi} increases with decreasing S_{wi} with an intercept of 38% at S_{wi} = 0%. This value may reflect the saturation in higher permeability rocks that have clay lined pores or fine pores that do not contribute to flow but retain water. Given time and at capillary equilibrium S_{wc} approaches and eventually equals S_{wi} but within the operationally defined flow limits of Qg/Qw > 99.99 the observed S_{wc} is always greater. In low permeability rocks S_{wi} increases and S_{wc} also increases with decreasing permeability and at $S_{wc} \approx S_{wi}$ when S_{wi} = 100%.

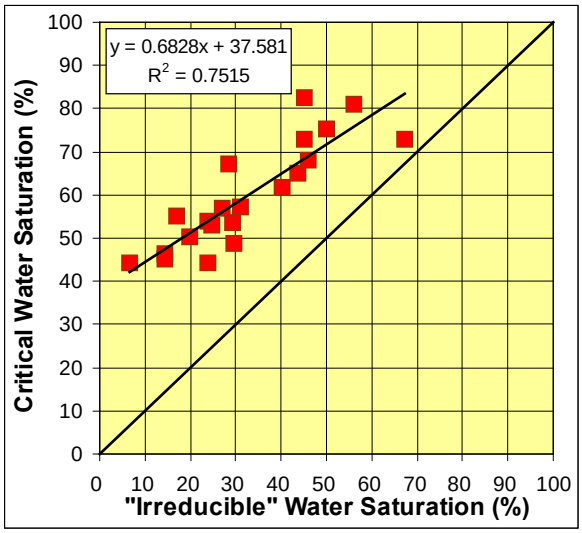

Fig. 4. *Critical water saturation (S_{wc}) versus "irreducible" water saturation (S_{wi}) as measured by air-brine capillary pressure analysis at 300 psia. The higher S_{wc} compared with S_{wi} values may indicate flow is concentrated in a small fraction of large pores and/or with increasing permeability water can occupy small pores without interfering with flow. The trend line through the data represents equation 11 in the text.*

The above results illustrate the potential disconnect between operational definitions for flow and capillary pressure equilibrium. These issues arise in the values used in the Corey equation. It might be thought that the issue can be resolved by simply redefining the $S_{wc} = S_{wi}$, i.e., the S_{wc} is defined as the minimum S_w (presumably S_{wi}) observed by any measurement method. This would resolve the problem except that S_{wi} must, in turn, be operationally defined at some specific capillary pressure. For high permeability rocks the concept of S_{wi} is useful and measured S_{wi} remains the same for the range of capillary pressures of interest in a reservoir system. In low-permeability sandstone systems this is not the case. These rocks are in their transition zone over intervals of hundreds to thousands of feet. As a result, S_{wi} must be operationally defined as representing the S_w at a specified capillary pressure or gas column height. Specification of a greater or lesser pressure results in "irreducible" saturations that can differ significantly.

To model water relative permeability equation 6 was used to define the k_{rw} (relative to k_{ik}) at S_w=1, equations 10 and 11 were use to model S_{wc} and a value of q = 4 was used to estimated k_{rw} using equation 7. Figure 5 illustrates the resulting k_{rw} curves for sandstones of different absolute permeability. For a water saturation somewhat typical of low-permeability rocks, S_w= 0.50, k_{rw} = 8e-5 for a 0.1 mD rock and k_{rw} < 1e-6 for a 0.01 mD rock. These very low relative permeabilities are consistent with the dry gas production of low-permeability rocks. Note that because water permeability, k_w, decreases with decreasing k_{ik}, k_{rw} decreases with decreases k_{ik}. In addition, because S_{wi} and S_{wc} increase with decreasing k_{ik}, k_{rw} further decreases with decreasing k_{ik}. The k_{rw} curves shown for higher permeability rocks (k_{ik} > 1 mD) represent less argillaceous lithologies. If clays are present in abundance both S_{wi} and S_{wc} increase above the values shown and correspondingly affect the k_{rw} curves.

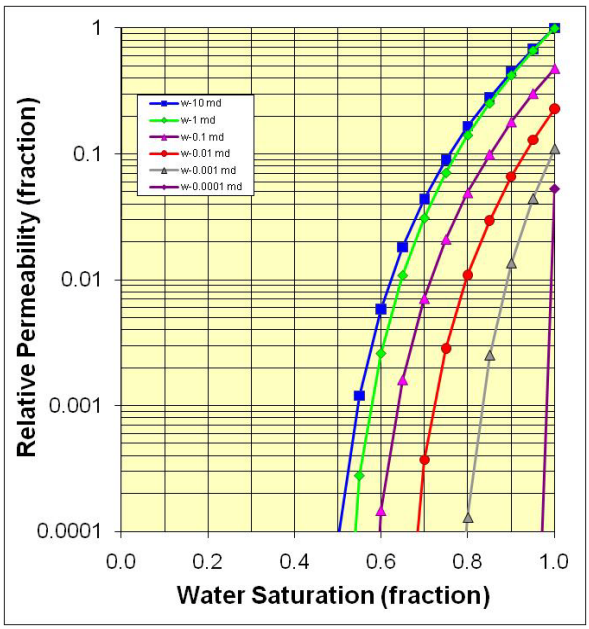

Fig. 5. *Water relative permeability curves for rocks of different absolute permeability estimated using equations 6, 7, 10, and 11 in the text.*

If it is assumed that critical water should be operationally defined as $S_{wc} \approx S_{wi}$ but that the Corey exponent q = 6, the water relative permeability curves take the form shown in Figure 6.

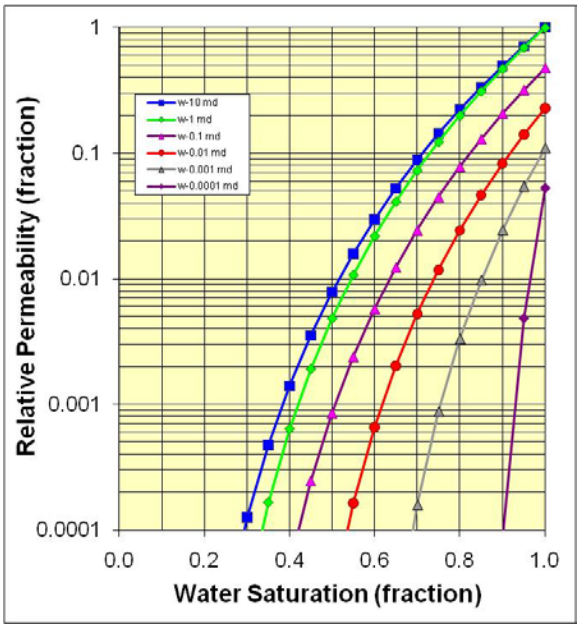

Fig. 6. *Water relative permeability curves for rocks of different absolute permeability estimated using equations 6, 7, and 10 in the text with $S_{wc} \approx S_{wi}$.*

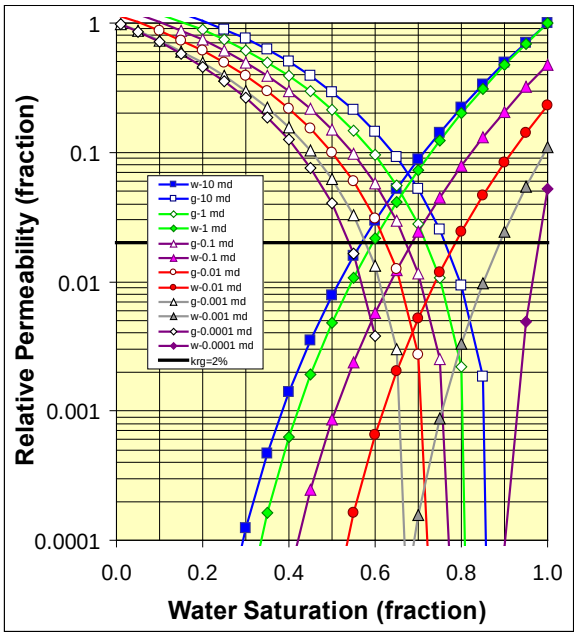

Fig. 7. *Gas (g) and water (w) relative permeability curves calculated using equations 1-5 for gas with p = 2 and eqns 6, 7, and 10 for water for a range of absolute permeabilities. Note crossover, where $k_{rg}=k_{rw}$ is approximately 67% for all permeabilities but k_{rg} value at crossover decreases with decreasing permeability. Dark black horizontal line marks the k_{rg} = 2% (0.02). The Sw region where both gas and water have k_r < 0.02 broadens as k_{ik} decreases.*

DRAINAGE PERMEABILITY JAIL

Applying equations 1-5 for gas and 6, 7, and 10 for water, using p = 2 and q = 6, to rocks of absolute permeability, k_{ik}, ranging from 0.0001 mD to 10 mD, we obtain the suite of k_{rg} and k_{rw} curves shown in Figure 7. All curves are referenced to the *in situ* Klinkenberg permeability, k_{ik}. The figure shows that the k_{rg}/k_{rw} crossover (where values are equal) occurs at approximately S_w= 0.67 for all permeabilities, but the crossover shifts to progressively lower values of k_r with decreasing permeability. If clays are abundant, corresponding increase in S_{wc} would result in a shift to higher S_w for the k_{rg}/k_{rw} crossover.

As a consequence of decrease in k_{rg} at the crossover, the range of S_w over which both k_{rg} and k_{rw} are less than 2% broadens. Beginning with the crossover at $k_{rg}=k_{rw}$= 0.02 for a 0.1 mD rock the range of S_w in Permeability Jail (S_{wJ}) broadens as:

k_{ik} = 0.100 mD: $0.65<S_{wj}<0.67$ [12]
k_{ik} = 0.010 mD: $0.62<S_{wj}<0.78$ [13]
k_{ik} = 0.001 mD: $0.55<S_{wj}<0.89$ [14]
k_{ik} = 0.0001 mD: $0.52<S_{wj}<0.98$ [15]

From these relations it is evident that in very low permeability rocks the saturation range over which the relative permeability to both phases is low and flow is restricted increases in width sufficiently to encompass nearly all S_w > 55%.

Figure 7 illustrates relative permeability for both phases but does not express the significant influence of the viscosity difference between the two phases. At pressure and temperature conditions very generally representative of tight gas sandstone reservoirs (Pressure = 5,000 psi, Temperature = 190 °F), the viscosity of gas (μ_g) is approximately μ_g = 0.02 centipoise (cp) and of water is μ_w = 0.5 cp. Rescaling Figure 7 to represent the relative permeability relative mobility (k_{rg}/μ_g and k_{rw}/μ_w) and maintaining gas flow as the reference frame provides insight on the relative flow of each phase and illustrates how low gas viscosity allows gas flow to dominate these systems (Fig. 8).

Figures 7 and 8 illustrate how low-permeability rocks at water saturations greater than ~50% can get into Permeability Jail. It is important to note that "Jail" does not mean that these rocks have no flow. As with Corey's original definition, Jail defines the condition where these rocks have no commercially significant flow. We explore how the genesis of how these rocks were sentenced to Jail below.

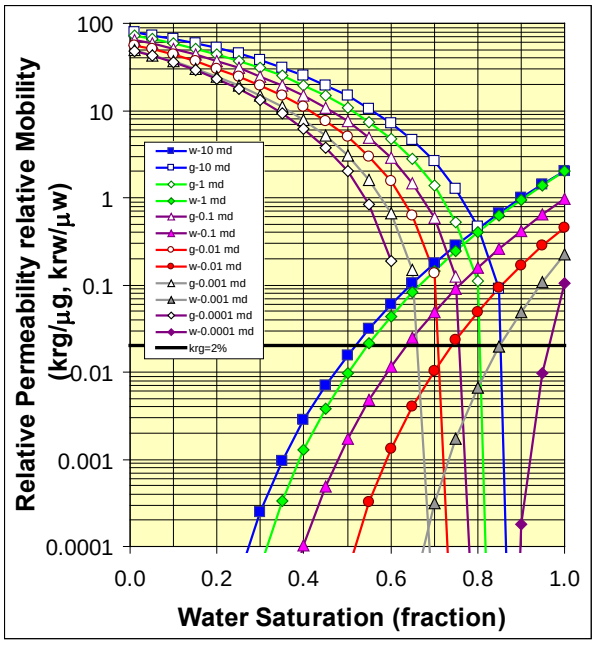

Fig. 8. *Gas (g) and water (w) relative mobility curves calculated using equations in the text for relative permeability as in Figure 8 but divided by the approximate viscosity of the fluids at reservoir conditions (gas = 0.02 centipoise, water = 0.5 centipoise) and referenced to the gas permeability. This figure illustrates the significant effect of viscosity on relative flow and illustrates why water production rates are so low compared to gas.*

IMBIBITION PERMEABLITY JAIL

Just as gas-brine drainage conditions can leave some low-permeability rocks in Permeability Jail, imbibition can also create Jail conditions. In air-mercury imbibition capillary pressure experiments on Mesaverde Fm. low-permeability sandstones we investigated residual non-wetting phase saturation (equivalent to gas saturation) by injecting mercury into samples to an initial non-wetting phase saturation and then measuring the residual mercury saturation following equilibrium imbibition capillary pressure decrease back to zero capillary pressure (Byrnes et al, 2009). Figure 9 illustrates the relationship between residual non-wetting phase saturation and the initial non-wetting phase saturation for the samples measured in the Byrnes et al (2009) study. The relationship between initial and residual non-wetting phase saturation was consistent with the relation characterized by Land (1971) for strongly water wet samples:

$$1/S_{nwr}^* - 1/S_{nwi}^* = C \qquad [16]$$

where $S_{nwr}^* = S_{nwr}/(1-S_{wi})$ and $S_{nwi}^* = S_{nwi}/(1-S_{wi})$.

For their samples a Land constant of C = 0.55 assuming S_{wirr} = 0 resulted in the minimum error in estimated residual saturation.

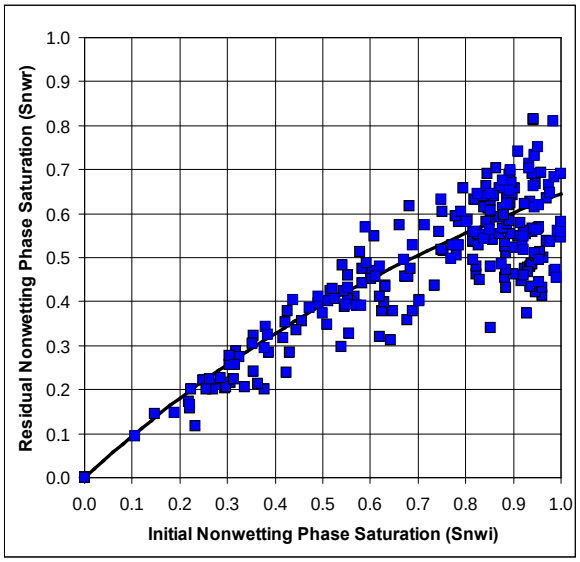

Fig. 9. *Cross-plot of residual and initial non-wetting phase (mercury) saturation for Mesaverde low-permeability sandstone. The black trend line represents a Land constant C=0.55 with S_{wi}=0 used in equation 16.*

The high residual saturations observed for these rocks are consistent with large pore bodies connected by thin tabular pore throats as described above. With large pore body to pore throat size ratios trapping by snap-off of the non-wetting phase in the pore bodies is expected. By definition the residual saturations in these experiments represents an immobile phase, thus imbibition forced the non-wetting phase (here mercury but assumed to be representative of gas also) into Permeability Jail.

These experiments did not utilize brine or measure flow. However, commonly imbibition relative permeability to brine at the wetting-phase saturation associated with residual non-wetting phase $k_{rw,1-Snwr}$, ranges from values of $0.1 < k_{rw} < 0.5$ and always satisfies the condition that $k_{rw,1-Snwr} < k_{rw}$. Therefore, for imbibition conditions, higher permeability rocks that might not be in Drainage Permeability Jail could be in Imbibition Permeability Jail, depending on the initial gas saturation and the imbibition capillary pressure, which would control the residual gas saturation.

HYSTERESIS PERMEABILITY JAIL – OR THE PERMEABILITY FUNNY FARM

Even rocks that might not be sentenced to Permeability Jail may end up in the Permeability Funny Farm if they

become "hysterical". Within the tall transition zone of many low-permeability rocks change in pressure and pore geometry as the result of diagenesis can result in drainage-imbibition cycling and potential drainage-imbibition hysteresis (Shanley et al, 2007). That is, trapping, which is different from the equilibrium imbibition trapping described above, may occur due to isolation of regions of the pore space as the result of rate-dependent fluid movement and potential trapping in regions that under equilibrium imbibition conditions might not experience the same amount of trapping. Obviously this would be more likely in lithologies with complex pore geometries.

We do not know of any published studies that experimentally test gas-brine drainage-imbibition hysteresis. It can be hypothesized that that this system might be intermediate between the drainage and imbibition Permeability Jail conditions, but hysteresis opens up the possibility that on a larger scale there may be trapping and that larger regions of rock may be in Permeability Jail simply because surrounding rocks entered Permeability Jail during some drainage or imbibition cycle.

THE PERMEABILITY JAIL GARDEN

The conditions described above address scales applicable to the scale of measurement of the relative permeability curve or, as above, a larger scale trapping phenomenon. In any good jail there should be a garden. It is also possible to have rocks enter the Permeability Jail garden as the result of internal gas generation and the creation of isolated gas-filled pores. Many low-permeability sandstones contain organic macerals, often coaly fragments, at concentrations as great as 0.5-1% total organic carbon. During burial these macerals, just as with coal, undergo organic diagenesis and generate gas. Because these macerals are small and dispersed through the rock, the gas generated may saturate surrounding brine and then fill surrounding pores with free gas. If this gas does not reach the percolation threshold or critical gas saturation we would observe potentially high gas saturations but relative gas and water permeabilities in the Permeability Jail region.

Byrnes (2007) reviewed aspects of critical gas saturation as applied to low-permeability sandstones. The majority of critical-gas saturation studies have focused on modeling S_{gc} in solution-gas-drive oil reservoirs where gas saturation is achieved by gas nucleation resulting from pressure decline and gas bubble growth within a network of variable pore size and connectivity. Solution-gas laboratory-measured S_{gc} values have ranged from 0.006 to 0.38 (Hunt and Berry, 1956; Handy, 1958; Moulu and Longeron, 1989; Kortekaas and Poelgeest, 1989; Firoozabadi et al., 1989; and Kamath and Boyer, 1993). Wilkinson and Willemsen (1983) showed that the volume fraction of the percolation threshold, equivalent to S_{gc}, scales with network dimension, L, as:

$$S_{\mathrm{gc}}(L) = \mathrm{A}\, L^{D-E} \qquad [17]$$

where A is a numerical constant, D is the mass fractal dimension of the percolation cluster (D = 1.89 for 2-D, D = 2.52 for 3-D), E is the Euclidean dimension (E = 2 for 2-D and E = 3 for 3-D). For a simple 3-D cubic network A ≈ 0.65. This relation indicates that as $L \rightarrow \infty$ $S_{gc} \rightarrow 0$ (e.g., S_{gc} = 0.215 for L = 10; S_{gc} = 0.024 for L = 1,000; S_{gc} = 0.008 for L = 10,000).

Li and Yortsos (1993, 1995a) and Du and Yortsos (1999) extended the invasion percolation work to include gas nucleation at one or more sites showing that S_{gc} scales with network size, L, and the fraction of total network sites where gas nucleation occurs, f, as:

$$S_{gc}(L; fq) = \mathrm{A}\, L^{D-E} + \mathrm{B}\, f^{1-D/E} \qquad [18]$$

where A and B are numerical constants, D is the mass fractal dimension of the percolation cluster (D = 1.89 for 2-D OP, D = 1.82 for 2-D IP with trapping, D = 2.52 for 3-D OP or IP, with or without trapping), E is the Euclidean dimension (E = 2 for 2-D and E = 3 for 3-D), and f is the fraction of total network sites where gas nucleation occurs. In the limit of very small f (e.g., one nucleation site only or external drive) the second term is approximately zero and S_{gc} corresponds to the volume fraction of the percolation cluster only, as presented in Equation 17. When the nucleation fraction increases, the main contribution to S_{gc} results from clusters growing around nucleation sites and not from the percolation cluster (Du and Yortsos, 1999). For large networks the first term in Equation 18 vanishes and S_{gc} becomes primarily a function of the fraction of nucleation sites.

It is common that organic maceral content increases with decreasing depositional environment energy and therefore nucleated gas saturation is likely to increase with decreasing grain size and associated absolute permeability and possibly porosity. Assuming this model, it is likely that isolated nucleated gas saturation would be greater in rocks that might exhibit the poorest reservoir properties and lowest drainage gas saturations. Thus it could be hypothesized that rocks with progressively lower permeability would exhibit a potentially greater range of gas saturation, as a function of organic content and thermal maturity, which would place the rock in the Permeability Jail Garden.

L
L
L
L

JAIL GENESIS

The concept of Permeability Jail is independent of how these conditions came about. Therefore it is not necessary to know how a rock was sentenced to Jail, but it is nonetheless helpful to understand the genesis. A perceived issue with Permeability Jail is the question: If the gas permeability is zero how did the gas get into the rock in the first place? There are several answers to this question depending on how the rock was arrested. For the cases of Imbibition Jail and the Permeability Funny Farm the simple answer is the gas entered under normal drainage conditions and the rock entered Permeability Jail due to water imbibition or drainage-imbibition cycling with hysteresis. For rocks in the Permeability Jail Garden the gas was generated *in situ* and never "entered" the rock from an exterior source (invasion percolation) and so the rock started in Jail and remains in Jail. If the rock contains sufficient organic matter and is sufficiently thermally mature, then the nucleated gas sites would form a sample spanning percolating cluster and the rock would, with sufficient connected percolation sites, be released from Jail (early release for good behavior). Organic-rich gas shales represent an example of this condition for rocks of extremely low (<< 1 μD) permeability.

The answer for Drainage Jail is tied to definitions and time. As noted, and just as Brooks & Corey (1966) used the term, critical saturation is defined as the saturation at which no *significant* flow occurs. We define Permeability Jail as the saturation region in which no significant (i.e., *kr* < 2%) flow occurs. Here the criteria for significance are tied to laboratory and commercial field conditions. This does not preclude flow over long periods of time or even flow rates that are just sub-economic. For this condition, gas could enter a rock over geologic periods of times but flow on the scale of days-years would be considered insignificant. In addition, what is considered insignificant for one level of stimulation technology, such as vertical completion with a massive fracture, might be significant for another level of technology, such as a long-reach multi-fracture horizontal well with 20 stages. In effect, a rock can be bailed out of Jail if someone is willing to post the bond (and presumably expects to get their bond money back).

It is also possible for rocks in Permeability Jail to possess a "Get Out Of Jail Free' card. An example of this condition is a naturally fractured formation. Here the reservoir rock at the matrix scale is in Jail but the pseudo-permeability of the fracture-matrix system is not in Permeability Jail.

Finally, it is possible for a reservoir to have been gas charged early in its burial history, when rock properties were better, and with subsequent burial and diagenesis, the rock properties changed and the rock entered Permeability Jail. This condition may be the norm and not the exception. It is instructive to analyze this by briefly examining a theoretical burial scenario.

Let us assume the following conditions that are broadly representative of Western United States Mesaverde low-permeability sandstones:

Present: $\phi = 10^{(-0.000045\ \text{Depth(ft)} - 0.7)}$ (Fig. 10) [19]
S&C: $\phi = 10^{(-0.000036\ \text{Depth(ft)} - 0.31)}$ (Fig. 10) [20]
modS&C: $\phi = 10^{(-0.00004\ \text{Depth(ft)} - 0.36)}$ (Fig. 10) [21]
k_{ik} (mD) $= 10^{(30\ \phi_t - 4.7)}$ (Fig. 10) [22]
P_{gas} (psi) = 0.5 Depth (ft) [23]
T_{gas} (degF) = 55 + 0.015 Depth(ft) [24]
Capillary pressure curves (Fig.11) [25]

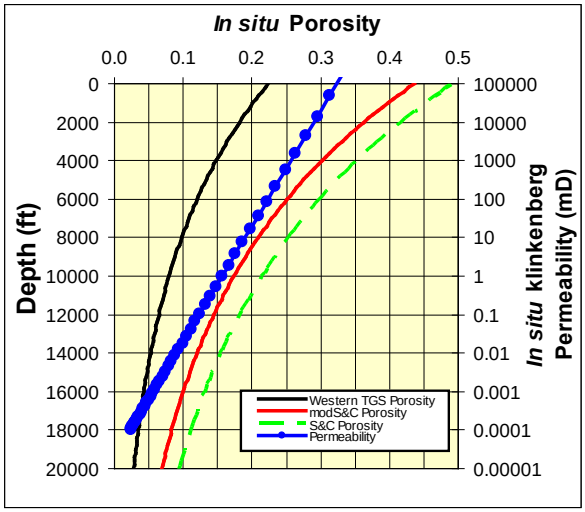

Fig. 10. *General trends for Western US low-permeability sandstones presented in equations 19-22.*

The porosity-depth relationship in equation 19 is generalized and represents observed trends for wells in the Greater Green River Basin, Wyoming, USA. This trend, however, is influenced by both removed overburden and diagenesis. Equation 20 is the porosity-depth trend reported by Sclater and Christie (1980) and Baldwin and Butler (1984) for North Sea sandstones of low thermal maturity and eq. 21 is a modified-Sclater and Christie (1980) trend for lithic sandstones. Though lithologic variability certainly influences these trends, it is hypothesized that the Western US Mesaverde sandstones followed a trend similar to the modified-Sclater and Christie (1980) porosity-depth trend (eqn. 21) early in their depositional history when they were thermally immature. During subsequent deeper burial increased time-temperature exposure caused porosity occlusion and at the final stage of burial prior to uplift and erosion the sandstones reached the present-day

porosity-depth (Eq. 19) trend and maintained the minimum porosity on uplift.

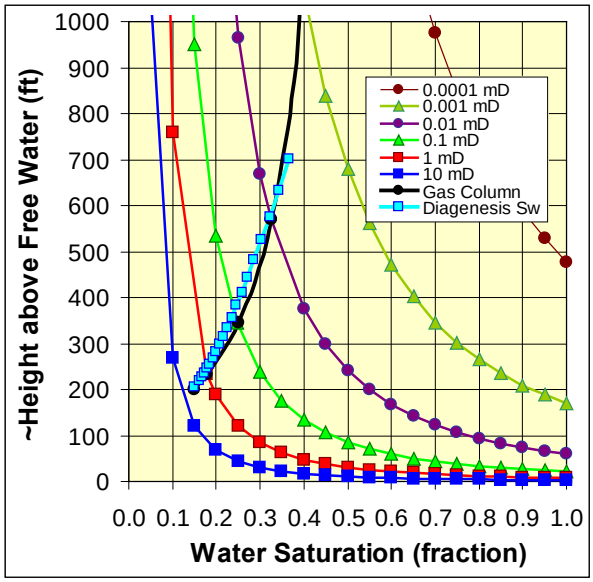

Fig. 11. *General capillary pressure curves for example low-permeability sandstones. Gas column height curve from capillary pressure relations shows height-saturations at top of column as discussed in text. Light blue squares show water saturation in original gas column rock after porosity occlusion at corresponding gas column height.*

Based on burial thermal history modeling of the Northern Green River basin, Wyoming, USA (Coskey, 2004), it is probable that underlying coals and organic shales reached peak gas generation at approximately 13,000-16,000 ft burial depths. Assuming, as an exploratory example model, that the reservoir rocks 2,000 to 5,000 feet shallower (~10,000 ft) were charged with gas migrating vertically upwards it is possible to model the development of the reservoir rocks and gas cap through a hypothetical burial history (Fig. 12).

Modeling of reaction kinetics suggests that gas is primarily expelled in a brief pulse when the source rocks reach their maximum burial depth and temperature, while only minor amounts of gas are generated and expelled during the long quiet period near maximum burial illustrated in Figure 12 (see, for example, figures 12 and 13 in Coskey, 2004). All burial history modeling packages, based on the kinetic theory of organic matter transformation, predict similar transformation histories for Type III kerogen. Once uplift begins and the source rocks cool, assumed to start at 10 Ma in Figure 12, gas generation effectively ceases as all C-C bonds that are capable of being broken at these temperatures had already been severed at the higher thermal stress conditions of deeper burial.

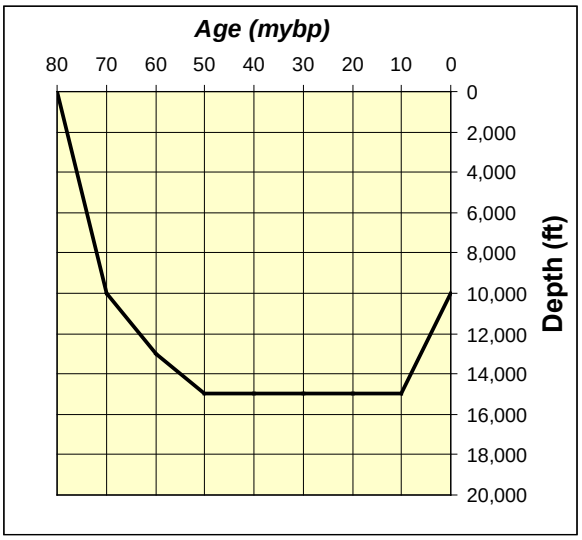

Fig. 12. *Theoretical burial history for a model Western US low-permeability sandstone. This burial history and the resulting change in properties described by equations 19-25 are used to model the evolution of a gas charged reservoir.*

Assuming eq. 21, the example reservoir sandstones at 10,000 ft at 70 Ma would have had ϕ =17.4% and from eq. 22 a permeability of 3.3 mD. It will be assumed that a gas reservoir with 200-ft of gas column was charged in a brief pulse and the subsequent conditions of this gas column will be examined. For the simple model being presented, it is further assumed that the mineral and water constituents are incompressible, therefore all porosity loss with depth that the reservoir experiences (Fig. 10) results in corresponding gas pore volume loss and consequent gas expulsion into underlying previously water-saturated rock. The gas is assumed to be pure methane and appropriate real gas laws apply for gas compressibility in response to increasing and decreasing pressure and temperature changes with burial and exhumation. Porosity destruction continues after the reservoir rocks have received their gas charge, at least in water wet reservoir systems. For the example model, porosity decrease with burial follows the modified-S&C curve to maximum burial depth at 15,000 ft (50 Ma). Porosity continues to occlude at this depth, approaching the present-day porosity, until 10 Ma when uplift and erosion bring the reservoir back up to a depth of 10,000 ft, leaving the reservoir with the present-day porosity at the present-day depth.

Gas in the model is conserved and water is assumed to be able to enter or leave the system to maintain equilibrium; consequently one of two things must occur. Either gas is expelled from the original reservoir as pore volume decreases, in which case (assuming a partially gas filled trap) the gas cap height increases (if

they are not conserved seal failure could result in gas expulsion at the top); or alternatively, in the case of a tightly sealed container the compressible gas will accommodate the porosity loss and the container will increase in pressure substantially. In at least the first case, assuming water is expelled out the bottom of the trap, the gas column will expand as the trapped gas volume is pushed into ever poorer quality rock. This scenario is investigated by the model.

Assuming gas moles are conserved then the volume of gas (V_g) is constant, if gas compressibility is ignored. If gas compressibility is considered during the burial history (Fig. 12), increasing pressure (P) and temperature (T) result in a net relative gas volume decrease from 1 (reference = 10,000 ft depth, P = 5,000 psi, and T = 204.8 °F) to 0.875 (depth = 15,000 ft depth, P = 7,500 psi, and T = 280 °F). The porosity decrease (Fig. 10) and gas compression result in a net gas expulsion from the original 200-ft thick gas reservoir that increases the gas column from 200-ft to a successively increasing series of gas column heights in response to decreasing porosity, decreasing permeability, and increasing equilibrium capillary pressure-predicted water saturation. At any given depth, and corresponding porosity and permeability, gas column height can be estimated by integrating the gas volume defined by the capillary pressure curve that applies to rocks at that defined depth:

$$V_g\beta_g = \int_0^h S_g\,\phi\,(D, P, T)\,A\,dh \qquad [26]$$

Where V_g is the constant gas volume, h is the gas column height, S_g is the gas saturation for each height within the gas column defined by the capillary pressure curve for the rock of porosity, ϕ, at the specific depth (D), β_g is the relative gas compressibility at the P, T conditions at D, A is unit area. For all depths of burial V_g is the same. Equation 26 is solved for the h for the conditions at each burial depth. Figure 13 illustrates the estimated gas column heights associated with selected porosities and corresponding permeabilities. Figure 14 illustrates the history of key reservoir properties.

To follow the gas reservoir history, the reservoir is charged at ϕ = 17.4%. With burial the porosity decreases, according to eq. 21, to ϕ = 11% at 15,000 ft. This loss in porosity results in compaction to 92.7% of initial reservoir thickness. With the porosity loss there is a corresponding permeability decrease from the initial 3.3 mD to 0.037 mD. This permeability decrease reflects a similar change in the capillary pressure curve to a curve intermediate between 0.01 mD and 0.1 mD (Fig. 11). In response to porosity and loss and capillary pressure change, at this depth the gas column height increased from 200 ft to 411 ft.

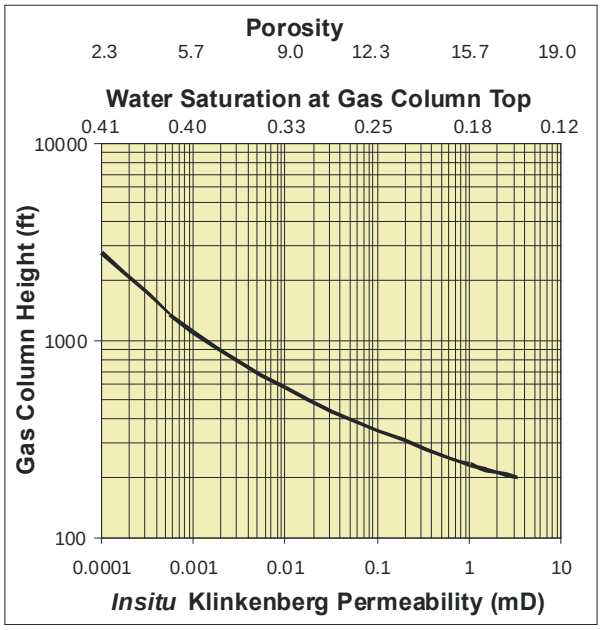

Fig. 13. *Estimated gas column heights based on porosity-depth trend in eq. 21, permeability in eq. 22, capillary pressure curves in Fig. 12, and eq. 26 for an initial gas column height of 200 ft charged at a depth of 10,000 ft.*

Following burial to 15,000 ft the reservoir remained at this depth, pressure, and temperature for 40 My. During this time porosity occlusion continued and porosity decreased from ϕ = 11% to ϕ = 7.8%. This porosity loss resulted in the following properties changes; S_w at top of column = 0.37, k_{ik} = 0.0048 mD, gas column height = 700-ft.

With uplift and erosion of 5,000 ft in the last 10 Ma, the reservoir was elevated back to a depth of 10,000 ft. At this depth, equilibrium pressure and temperature were reduced. It is assumed that diagenesis effectively stopped and porosity, permeability, and water saturation remained constant at the values they exhibited at 15,000 ft and 10 Ma [In fact, there is a slight dilation of porosity as a consequence of uplift and the reduction in net confining stress (NCS). We estimate this effect would be less than 0.5% for 10% porosity sandstone uplifted by 5,000 ft. With the increase in porosity there will also be a slight improvement in permeability, which we neglect for this example.] The reduction in pressure and temperature of the gas, under equilibrium conditions, would have resulted in a final gas expansion to an approximate gas column height of 800 ft. If the gas column was not able to expand in the time available and was not in capillary equilibrium, then the pressure in the gas, relative to the depth, would be overpressured at a gradient of approximately 0.75 psi/ft.

Figure 11 shows that the saturations achieved by diagenetic porosity occlusion and those consistent with capillary equilibrium for the same rocks are identical within the accuracy of the modeling. This would indicate that the upper 200-ft of the reservoir that represents the initial gas cap undergoes porosity occlusion and corresponding saturation change without imbibing or expelling significant amounts of water. This process for increasing water saturation by porosity occlusion does not conform to conventional imbibition conditions, where water saturation is increasing by invasion. It is surmised that under these conditions the gas would maintain connectivity, similar to water isotherm curves, and that this saturation change may be similar to drainage conditions in its flow properties.

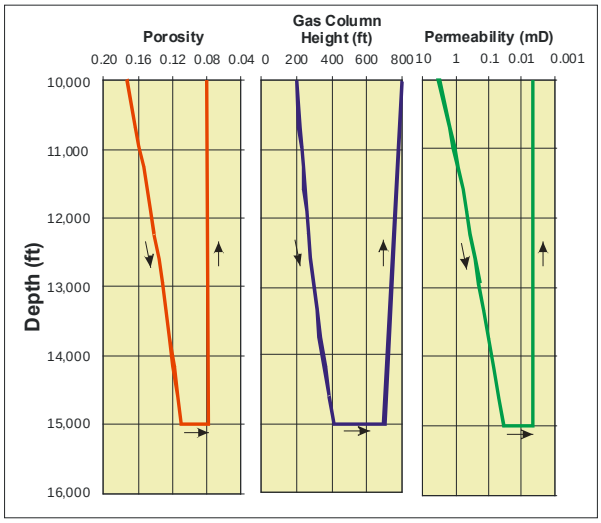

Fig. 14. *History of key reservoir properties following initial charge of a 200-ft high gas column at 10,000 ft and through burial to 15,000 ft and subsequent uplift to 10,000 ft. Arrow show direction of change resulting from burial and diagenesis.*

Figure 11 can be interpreted to show that the upper portion of the reservoir, representing the original gas cap, remains at sufficiently low water saturations that it does not enter Permeability Jail. However, with decreasing permeability, significant portions of the deeper part of the newly created gas column exhibit properties that are consistent with Permeability Jail. For sandstone with k_{ik} = 0.001 mD the gas column below 550 ft above free water level, representing approximately 42% the total gas column, is in Permeability Jail. For sandstone with k_{ik} = 0.01 mD the column below 200 ft above free water level, representing approximately 35% of the total gas column, is in Permeability Jail. Although it was not included in the above modeling, if gas generation were to continue during the events outlined above, the gas column would grow additional as a function of the volume of new gas added to the system. The additional height produced by the new gas would depend on the porosity and water saturations existing at the time of gas influx.

It is evident from the above example model history that the gas reservoirs undergo significant change with burial and diagenesis and that the changes to the gas column height and simultaneous changes to the porosity and permeability of the reservoir rocks result in progressively increasing gas column heights in which the lower-most portions of the columns are in conditions consistent with drainage Permeability Jail. As noted previously, the gas was allowed to enter rocks in Permeability Jail because the time periods for flow are so long that "insignificant" flow on a commercial time scale is significant in establishing the gas column on a geologic time scale.

CONCLUSIONS

The Permeability Jail model provides utility in understanding and modeling effective gas and water permeabilities in low-permeability sandstones. In rocks with permeability greater than 1 mD, relative permeability changes as a function of permeability are small and are more sensitive to lithology and saturation history. As permeability decreases below approximately 1 mD the changes in pore architecture to large isolated pore bodies separated by progressively increasing in length and narrowing in width tabular pore throats appear to cause systematic changes in the relative permeability. Most sandstone relative permeability work has been done over a comparatively narrow permeability range of two orders of magnitude (10-1,000 mD) where pore architectures are similar. In contrast the low permeability sandstones span four orders of magnitude in permeability (0.0001 – 1 mD) and exhibit a wide range in, and changing, pore geometry. Permeability Jail is simply a reflection of the systematic changes that occur in gas and water relative permeability with decreasing absolute permeability and as a function of saturation history. Data show that gas relative permeability decreases with decreasing absolute permeability. This shift is consistent with either a low S_{gc} and increasing Corey exponent p or with an increasing S_{gc} and constant p. It is probable that both conditions exist depending on lithology. Absolute water permeability decreases with decreasing absolute Klinkenberg permeability and S_{wc} increases with decreasing absolute permeability. The systematic changes in gas and water relative permeability properties with decreasing absolute permeability create a successive decrease in the relative permeability of the gas-water relative permeability cross-over. This

decrease, in turn, results in a progressively widening saturation range over which the relative permeability to both phases is less than a reference value of k_r < 2% - the rocks enter Permeability Jail. Several saturation history conditions can create conditions for Permeability Jail including drainage (Drainage Jail), imbibition (Imbibition Jail), drainage-imbibition hysteresis (Permeability Funny Farm), and nucleated percolation (Jail Garden). These informal designations are meant to portray with a little levity, but with accuracy and in a memorable fashion, what is a significant issue in low-permeability reservoir rock properties. Porosity, permeability, and capillary pressure changes a rock undergoes during burial and diagenesis can result in gas column height increase with significant (30-42%) portions of the lower portion of the gas column exhibiting conditions consistent with Permeability Jail. These concepts help to understand and explain the thick gas columns in western U.S. low-permeability sandstones and their diminished effective gas permeabilities.

REFERENCES

Baldwin, B., and Butler, C.O., 1985, Compaction Curves: American Association of Petroleum Geologists Bulletin, v. 69, n. 4, p. 622-626.

Brooks, R.H., and A.T. Corey, 1966, Properties of porous media affecting fluid flow: Journal Irrigation Drainage Division, v. 6 (June 1966), p. 61-88.

Byrnes, A. P., 1997, Reservoir characteristics of low-permeability sandstones in the Rocky Mountains: The Mountain Geologist v. 43, no. 1, p. 37-51.

Byrnes, A.P., 2003, Aspects of Permeability, Capillary Pressure, and Relative Permeability Properties and Distribution in Low-Permeability Rocks Important to Evaluation, Damage, and Stimulation: Proceedings Rocky Mountain Association of Geologists - Petroleum Systems and Reservoirs of Southwest Wyoming Symposium, Denver, Colorado, September 19, 2003, 12 p.

Byrnes, A.P., 2005, Permeability, capillary pressure, and relative permeability properties in low-permeability reservoirs and the influence of thin, high-permeability beds on production: *in* M.G. Bishop, S.P. Cumella, J.W. Robinson, and M.R. Silverman (eds.), Gas in Low Permeability Reservoirs of the Rocky Mountain Region, Rocky Mountain Assoc. of Geologists 2005 Guidebook CD, p. 69-108.

Byrnes, A. P., 2008, Issues with gas relative permeability in low-permeability sandstones: *in* S.P. Cumella, K.W. Shanley, and W. Camp (eds.), Understanding, exploring, and developing tight-gas sands – 2005 Vail Hedberg Conference, American Association of Petroleum Geologists Hedberg Series n. 3, Chapter 5, p. 63-76.

Byrnes, A.P., and J.W. Castle, 2000, Comparison of core petrophysical properties between low-permeability sandstone reservoirs: Eastern U.S. Medina Group and Western U.S. Mesaverde Group and Frontier Formation: paper SPE 60304, Proceedings of the 2000 SPE Rocky Mountain Regional/Low Permeability Reservoirs Symposium, Denver, CO, March 12-15, 2000, 10 p. DOI: 10.2118/60304-MS.

Byrnes, A.P., R.M. Cluff, and J.C. Webb, 2009, Analysis of Critical Permeability, Capillary and Electrical Properties for Mesaverde Tight Gas Sandstones from Western U.S. Basins, U.S. Department of Energy Final Report Project # DE-FC26-05NT42660; 355 pgs, http://www.kgs.ku.edu/mesaverde/reports.html,

Byrnes, A. P., K. Sampath, and P.L. Randolph, 1979, Effect of pressure and water saturation on the permeability of western tight sandstones: Proceedings of the 5th Annual U.S. Dept. Energy Symposium on enhanced oil and gas recovery, Tulsa, Oklahoma, August 22-26, 1979, p. 247-263.

Castle, J.W., and Byrnes, A.P., 1998, Petrophysics of low-permeability Medina Sandstone, northwestern Pennsylvania, Appalachian Basin: paper SPWLA 1998-v39n4a3, The Log Analyst, v. 39, no. 4, p. 36-46.

Castle, J.W., and A.P. Byrnes, 2005, Petrophysics of Lower Silurian sandstones and integration with the tectonic-stratigraphic framework, Appalachian basin, United States: American Association of Petroleum Geologists Bulletin, v. 89, no. 1 (January 2005), p. 41-60. DOI: 10.1306/080170404028.

Cheng, C.H., and Toksoz, M.N., 1979, Inversion of seismic velocities for the pore aspect ratio spectrum of rock: Journal of Geophysical Research, v. 84, n. B13, p. 7533-7544.

Chowdiah, P., 1987, Laboratory measurements relevant to two-phase flow in a tight gas sand matrix: paper SPE 16945-MS, Proceedings of the 62nd Annual Technical Conference and Exhibition of the Society of Petroleum Engineers, Dallas, Texas, September 27-30, 12 p. DOI: 10.2118/16945-MS.

Corey, A.T., 1954, The interrelations between gas and oil relative permeabilities: Producers Monthly, v. 19 (Nov 1954), p 38-41.

Coskey, R.J., 2004, Burial-history modeling of the Jonah Field Area: an unusual and possibly unique gas accumulation in the Green River Basin, Wyoming, *in* J.W. Robinson and K.W. Shanley, eds., Jonah Field: case study of a tight-gas fluvial

reservoir: AAPG Studies in Geology 52, Ch. 7. P. 93-125.

Du, C., and Y.C. Yortsos, 1999, A numerical study of the critical gas saturation in a porous medium: Transport in Porous Media, v. 35, n. 2, p. 205-225. DOI: 10.1023/A:1006582222356.

Firoozabadi, A., B. Ottesen, and M. Mikklesen, 1989, Measurement and modeling of supersaturation and critical gas saturation: Part 1. Measurements: paper SPE 19694, Proceedings of the 1989 Soc. Petroleum Engineers Fall Meeting, San Antonio, Texas, Oct. 8-11. DOI: 10.2118/19694-PA.

Handy, L. L., 1958, A laboratory study of oil recovery by solution gas drive: paper SPE 797-G, Petroleum Transactions AIME, v. 213, p. 310-315.

Hunt, E. B., Jr. and V.J.Jr. Berry, 1956, Evolution of gas from liquids flowing through porous media: American Institute of Chemical Engineering Journal, v. 2, n. 4, p. 560-567. DOI: 10.1002/aic.690020426.

Jones, F. O., and W.W. Owens, 1980, A laboratory study of low-permeability gas sands: paper SPE 7551-PA, Journal of Petroleum Technology, v. 32, no. 9, p.1631-1640. DOI: 10.2118/7551-PA.

Kamath, J. and R.E. Boyer, 1993, Critical gas saturation and supersaturation in low permeability rocks: paper SPE 26663, Presented at the 1993 Society of Petroleum Engineers Fall Meeting, Houston, TX, Oct. p. 3-6. DOI: 10.2118/26663-PA.

Kamath, J. and R. E. Boyer, 1995, Critical Gas Saturation and Supersaturation in Low-Permeability Rocks: SPE 2663-PA, Society of Petroleum Engineers Formation Evaluation, v. 10, n. 4, p. 247-254. DOI: 10.2118/26663-PA.

Kortekaas, T.F.M., and F.V. Poelgeest, 1989, Liberation of solution gas during pressure depletion of virgin and watered-out reservoirs: paper SPE 19693, Presented at the 1989 Fall Meeting of the Society of Petroleum Engineers, San Antonio, Texas, Oct. 8-11. DOI: 10.2118/19693-PA.

Land, C.S., 1971, Comparison of Calculated with Experimental Imbibition Relative Permeability: paper SPE 3360-PA, Society of Petroleum Engineers Journal, v. 11, n. 4, p. 419-425. DOI: 10.2118/3360-PA.

Li, X. and Y.C. Yortsos, 1993, Critical gas saturation, modeling and sensitivity studies: paper SPE 26662-MS, Proceedings of the 68th Annual Technical Conference of the Soc. Petroleum Engineers, Houston, Texas, Oct. 3-6, p. 589-604. DOI: 10.2118/26662-MS.

Li, X., and Y.C. Yortsos, 1995a, Theory of multiple bubble growth in porous media by solute diffusion: Chem. Engineering Science, v. 50, n. 8, 1247-1271. DOI: 10.1016/0009-2509(95)98839-7.

Luffel, D.L., Howard, W.E., and Hunt, E.R., 1991, Travis Peak core permeability and porosity relationships at reservoir stress: paper SPE 19008-PA, Society of Petroleum Engineers Formation Evaluation, September, 1991, v. 6, n. 3, p. 310-319. DOI: 10.2118/19008-PA.

Moulu, J. C. and D. Longeron, 1989, Solution-gas drive: experiments and simulation: Journal of Petroleum Science & Engineering, Paper presented at the Fifth European Symposium on Improved Oil Recovery, Budapest, Hungary, v. 2, n. 4, p. 379-386.

Ostensen, R. W., 1983, Microcrack permeability in tight gas sandstone: paper SPE 10924-PA, Society of Petroleum Engineering Journal, v. 23, no. 6, p. 919-927. DOI: 10.2118/10924-PA.

Randolph, P.L., 1983, Porosity and permeability of Mesaverde sandstone core from the U.S. DOE Multiwell Experiment, Garfield County, Colorado: paper SPE 11765-MS, Proceedings 1983 SPE/DOE Joint Symposium on low permeability gas reservoirs, March 13-16, 1983, Denver, CO, p. 449-460. DOI: 10.2118/11765-MS.

Sampath, K., and C.W. Keighin, 1981, Factors affecting gas slippage in tight sandstones: paper SPE 9872, Proceedings of the 1981 SPE/DOE Symposium on Low Permeability Gas Reservoirs, Denver, CO, May 27-29 (1981) p. 409-416. DOI: 10.2118/9872-PA.

Sclater, J.G., and P.A.F. Christie, 1980, Continental stretching: an explanation of the post-mid-Cretaceous subsidence of the central North Sea basin: Journal of Geophysical research, v. 85, p. 3711-3739. DOI: 10.1029/JB085iB07p03711.

Shanley, K.W., R.M. Cluff, and J.W. Robinson, 2004, Factors controlling prolific gas production from low-permeability sandstone reservoirs: Implications for resource assessment, prospect development, and risk analysis, American Association of Petroleum Geologists Bulletin, v. 88, no. 8, p. 1083-1121. DOI: 10.1306/03250403051.

Shanley, K.W., R.M. Cluff, and J.W. Robinson, 2007, Prolific gas production from low-permeability sandstone reservoirs - Part II: Reconciling basin history, fluid saturations, gas shows, and capillary pressure: AAPG 2007 Annual Convention, Long Beach, CA, Search and Discovery Article #110042.

Thomas, R. D., and D.C. Ward, 1972, Effect of overburden pressure and water saturation on gas permeability of tight sandstone cores: paper SPE 3634-PA, Journal of Petroleum Technology, v. 25, no. 2, p.120-124. DOI: 10.2118/3634-PA.

Vairogs, J., Hearn, C. L., Dareing, D. W., and Rhoades, V. W., 1971, Effect of rock stress on gas production for low-permeability rocks: Journal of

L
L
L
L

Petroleum Technology, v. 24, no. 9, p. 1161-1167. DOI: 10.2118/3001-PA.

Walls, J.D., 1981, Tight gas sands: permeability, pore structure and clay: paper SPE 9871-PA, Proceedings of the 1981 SPE/DOE Symposium on Low Permeability Gas Reservoirs, Denver, CO, May 27-29 (1981) p. 399-409. DOI: 10.2118/9871-PA.

Walls, J.D., Nur, A.M., and Bourbie, T., 1982, Effects of pressure and partial water saturation on gas permeability in tight sands: experimental results: paper SPE 9378-PA, Journal of Petroleum Technology, v. 34, n. 4, p. 930-936. DOI: 10.2118/9378-PA.

Ward, J.S., and N.R. Morrow, 1987, Capillary pressure and gas relative permeabilities of low permeability sandstone: paper SPE 13882-PA, Society of Petroleum Engineers Formation Evaluation, Sept. 1987, p. 345-356. DOI: 10.2118/13882-PA.

Wei, K.K., Morrow, N.R., and Brower, K.R., 1986, Effect of fluid, confining pressure, and temperature on absolute permeabilities of low permeability sandstones: paper SPE 13093-PA, SPE Formation Evaluation, v. 1, n. 4, p. 413-423. DOI: 10.2118/13093-PA.

Wilkinson, D., and J.F. Willemsen, 1983, Invasion percolation: a new form of percolation theory: Journal Physics A: Mathematical General, v. 16, p. 3365-3376. DOI: 10.1088/0305-4470/16/14/028.

ABOUT THE AUTHORS

Robert Cluff received his BS and MS degrees in Geology from the University of California at Riverside and University of Wisconsin at Madison. He later studied geology at the University of Illinois Urbana-Champaign and recently added a BA in Mathematics at Metro State College of Denver to his resume. Bob has been very active in SPWLA over the years including serving as North American Regional Director, VP of Membership and Administration, VP of Technology, and President of the Denver Well Logging Society. Bob started The Discovery Group, a Denver based geoscience and petrophysics consultancy, in 1987. Discovery Group is best known for their work in tight gas sandstone and shale gas reservoirs worldwide.

Alan Byrnes received his BS in Geology from the University of Illinois at Chicago and his MS in Geophysical Sciences from the University of Chicago. He has worked as a Research Geologist, Core Petrophysicist, and Project Manager at the Institute of Gas Technology, Marathon Oil Company Research Center, Core Laboratories, and Tetra Tech; owned and operated GeoCore, a special core analysis laboratory, for twelve years; was a Research Geologist at the Kansas Geological Survey for ten years and joined Chesapeake Energy as a Senior Petrophysicist in 2008. He has worked and published for 30 years on low-permeability rock properties, oil/gas field and laboratory studies, computer modeling, reservoir characterization and integration of geologic-petrophysical-engineering analysis.

Bob and Alan have been friends and colleagues for over 23 years and have collaborated on many public and proprietary studies throughout the US and other areas of the world. Their most recent collaboration was a major study of petrophysical properties of Mesaverde sandstones in several US basins which is available online at http://www.kgs.ku.edu/mesaverde/.

ACKNOWLEDGEMENTS

This work was supported in part under the U.S Department of Energy Contract # DE-FC26-05NT42660.

L
L
L
L